Experimentation and numerical analysis of the influence of geogrids with emulsion insertion on the behavior of bituminous pavements - Case of Ouargla aerodrome

●R. Bazine[a], ●M. Abdessemed[b]✉, ●S. Kenai[b] , ●N. Ouadah[b]

a. University of Kesdi Merbah of Ouargla, (Ouargla, Algeria)
b. Geomaterials and Civil Engineering Laboratory, University of Blida1, (Blida, Algeria)
✉: abdesmoul@yahoo.fr

ABSTRACT: This paper presents an experimental study on a set of 30 specimens, tested on three-point bending, divided into two categories. With the insertion of geogrids and cathodic emulsions, the first category consists of 14 prismatic beams and the second of 16 pre-cracked and reinforced slab specimens. In situ tests were carried out using a heavy deflectometer (HWD) on a flexible runway of an airfield located in the city of Ouragla (800 km south-east of Algiers), before and after its reinforcement. This work showed, with a numerical calibration, that the geogrid with emulsion, improves the displacements and the stresses approximately 30% and increases the modulus of elasticity and the modulus of rupture (MOR) by 60% and 20%, respectively. The damping coefficient (k) can reach the value of 2 to 5, which increases the longevity of a reinforced flexible pavement.

KEY WORDS: Pavement; Experimental; Modelling; Geogrid; HWD.

Citation/Citar como: Bazine R, Abdessemed M, Kenai S, Ouadah N. 2024. Experimentation and numerical analysis of the influence of geogrids with emulsion insertion on the behavior of bituminous pavements - Case of Ouargla aerodrome. Mater. Construcc. 74(353):e339. https://doi.org/10.3989/mc.2024.355723.

RESUMEN: *Experimentación y análisis numérico de la influencia de las geomallas con inserción de emulsión en el comportamiento de los pavimentos bituminosos - Caso del aeródromo de Ouargla.* Este trabajo presenta un estudio experimental sobre un conjunto de 30 probetas, ensayadas a flexión en tres puntos, divididas en dos categorías. Con la inserción de geomallas y emulsiones catódicas, la primera categoría consta de 14 vigas prismáticas y la segunda de 16 probetas de losa prefisurada y reforzada. Se realizaron ensayos in situ con un deflectómetro pesado (HWD) en una pista flexible de un aeródromo situado en la ciudad de Ouragla (800 km al sureste de Argel), antes y después de su refuerzo. Este trabajo demostró, con una calibración numérica, que la geomalla con emulsión, mejora los desplazamientos y las tensiones aproximadamente un 30% y aumenta el módulo de elasticidad y el módulo de rotura (MOR) en un 60% y un 20%, respectivamente. El coeficiente de amortiguamiento (k) puede alcanzar el valor de 2 a 5, lo que aumenta la longevidad de un pavimento flexible reforzado.

PALABRAS CLAVE: Pavimento asfáltico; Experimental; Modelización; Geomalla; HWD.

1. INTRODUCTION

The road network is an important development of any country. It has been reported that the lack of the road network in sub-Saharan Africa has increased the cost of goods by 30 to 50% (1). In Algeria, the road network is about 127 thousand km, of which almost 6,000 km are motorways, in addition to 36 airfields, almost 90% of the volume of economic exchanges (2). Most of the pavements are of the flexible asphalt type. Given the intensity of vehicle and machine traffic (for road runways) and aircraft traffic (for airport runways), as well as the environmental conditions, the loss of the structural characteristics of these pavements gives rise to deformations and degradations, which manifest themselves in the form of cracks propagating to the lower layers of these runways (3). In Saharan arid areas, where temperatures are high, reflective crackings are widespread, as these propagate from the running surface downwards into the pavement body, adversely affecting the lower sub-layers and considerably reducing the bearing capacity of the whole and accelerating the deterioration of the pavement body (Figure 1).

Figure 1. State of deterioration of asphalt pavement.

The literature has shown that the addition of surface layers (called overlay), can increase the structural capacity and reduce axial and tangential stresses, however this technique is costly and does not guarantee the non-failure of the pavement, especially in high temperatures areas and where rutting occurs (or the rutting spots) (4). For this reason, other methods of maintenance and rehabilitation of pavement structures are used, such as the technique of asphalt concrete with additives (BBA), either with special fibers (5), with high modulus asphalt concrete (HMAB), or even with cold recycled bonded materials (CRBMs) (6), in order to resist plastic deformation when heavy traffic increases (7). In the search for technologies that allow rapid repair and reinforcement, while improving the durability of the road surface, the innovative technique of applying geosynthetics, as materials that play the dual role of separation and reinforce-

ment, surfaced in the 1990s (8). This technique was applied, in addition to road and airport pavements with heavy traffic, to solve problems of drainage, subsidence, consolidation of subgrade soils and stability of railway platforms (9). More specifically, the types of geosynthetics, called "geogrids", have been successfully used to stabilize road, railway and airport sub-bases, as well as to delay cracking and apparent distress (10, 11). The effect of adding geogrids on the performance of asphalt concrete has been shown to be effective in reducing stresses and strains in flexible pavements (12). Most previous research has focused on the optimal choice of geogrid type and location to quantify its effectiveness in a flexible pavement structure (13). Full-scale tests have also been used to provide new insight into the quantification of geogrid effectiveness on flexible pavement performance (14).

However, few work have investigated simultaneously the optimal choice of the type and the best location of geogrids in the sub-base layers of the road or runway tested, taking into account the effect of the temperature and the size of the samples (specimens) tested and this paper propose to fill in this gap. This paper reports on the laboratory experimental investigation conducted on thirty specimens, divided into two categories. The first category consists of 14 specimens in the form of prismatic beams, of dimensions (305×90×70) mm, made of bituminous concrete mix designed according to the standards in force. While the second category is composed of 16 samples in the form of rectangular slabs of dimensions (500×180×100) cm, pre-cracked and tested in 3-point bending. This is a simulation of flexible pavements before and after their reinforcement with geogrid layers, with pre-cracking that allows the controlled propagation of the apparent crack during loading. The geosynthetics chosen (of the geogrid type) were manufactured and co-produced in Algeria, with a glass fibre composition (15).

The objective of this work is to analyse the influence and behavior of the use of geogrid reinforcement, as well as the attachment of emulsion, in a flexible pavement. Finite element numerical model was developed using a commercial software and the stresses and displacements were found comparable to the laboratory experimental results. The apparent crack growth rate and displacement at the base of the asphalt pavement were dependent on the value of the Young's modulus and influenced by the type of the geogrid used and the tack coat (16), as well as the percentage of emulsion applied. In addition, the value of this modulus (E) affects the vertical displacement of the bitumen pavement and the normal stress due to concrete loading (17). The high temperature, had an adverse effect on the mechanical performance of the geogrid-reinforced bituminous pavement of the runway. The insertion of the geogrid, with an emulsion layer at the interface, gives gains of up to 50% for stresses and nearly 20% for displacements, while

the pre-crack, with insertion of the geogrid layer with cathodic emulsion, improves the modulus of rupture (MOR) by around 10% and the damping coefficient (k) can range from 2 to 5, which increases the life of the reinforced asphalt pavement, by delaying upward cracking and reflection cracking. It was noted that the pseudo-dynamic HWD test made a positive contribution to the comprehension of the behavior of a flexible pavement in a hot clammy hot dry, area before and after reinforcement with geogrids (18).

2. EXPERIMENTAL PROGRAMME

2.1. Materials used in the laboratory

Bituminous concrete mixes were prepared to fabricate 30 specimens, divided into two categories of test specimens, were prepared, using two different types of geogrids and two types of emulsions different percentages. All these materials were chosen according to the test conditions and the equipment and instrumentation available in accordance with the standards in force (19).

2.1.1. Bituminous concrete

The composition of the asphalt concrete used to manufacture the test specimens was carried out according to the UNE-EN 13108-1 standard (20). After preliminary tests and in order to estimate the appropriate dosage, a formulation study mix design was carried out, using granular fractions of crushed sand (0/3), gravel in (3/8) and medium gravel (8/15). For pure 40/50 bitumen, the optimum bitumen content is 5.6%. (21). The dosage of binder applied was 800 g/m². It should be noted that the impregnation dosage is necessary due to the presence of the geogrid. According to EN 13285-3:2013 (22) and EN 13108-2:2013 (23), the dosage value varies between 600 and 800 g/m², which is recommended to ensure good adhesion between the applied geogrid and the bituminous concrete, especially in climatic conditions in arid zones, which favours the compensation for the evaporation.

2.1.2. Cationic emulsions

Two types of cationic emulsions, as a tack coat, usually used in practice during the construction and repair of road and airport pavements, were applied to the interface between the sub-layers of the laboratory-made specimens (24, 25). These were ECR 65% and ECR 69% emulsions, which have a low viscosity and a rapid rupture and contained a sufficient quantity of bitumen. The application temperature of the emulsion is generally between 60 and 80°C.

2.1.3. Reinforcing geogrids

Two types of geogrids with different properties from different manufacturers were used. The reason for choosing these two types over others is that they have been used in several airport and road pavement reinforcement projects in Algeria over the last ten years, in compliance with the relevant suppliers (26, 27). The first type is a geogrid composed of a reinforcing grid of E-glass cable, bonded to a polypropylene nonwoven called GEOTER FNG 50/50 (Figure 2a). The second type is a geogrid made of high modulus polyester and wrapped with a bituminous coating called HaTelit® C 40/17 (Figure 2b). Both types of geogrids were tested with a quality control to determine the mechanical characteristics of each. The two tests to be carried out are the tensile test of the wide strips, using the Instron 5900 universal tensile machine (Figure 3), located at the Algiers Public Works Control Centre (CTTP), according to the ISO-10319 standard (28), which determines the tensile strength in both directions and the test to determine the surface mass of the geosynthetic layers (according to the standard: ISO-9864) (29). The specification and test results for the two geogrids are given in Table 1.
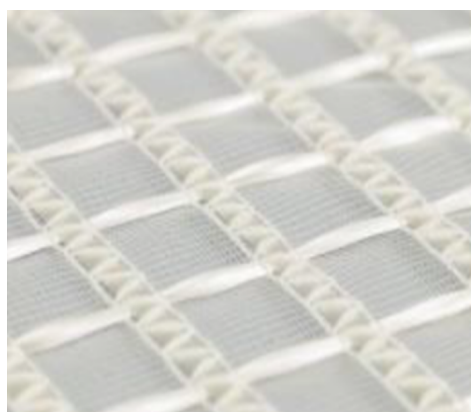
(a)	(b)

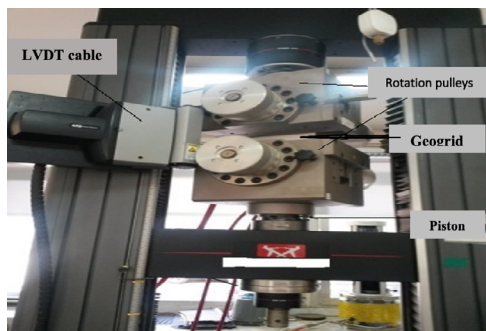**FIGURE 2.** a) Geogrid GEOTER FNG 50/50, b) Geogrid HaTelit® C 40/17.

FIGURE 3. Instron 5900 universal testing machine.

TABLE 1. Technical characteristics of the used geogrids.

Specification	Type1: GEOTER FNG 50/50	Type2: HaTelit® C 40/17
Tensile strength (kN/m) (longitudinal direction)	51.33	49.13
Tensile strength (kN/m) (tranversal direction)	55.03	56.64
Percentage of deformation at rupture	5.2%	5.6%
Materials	E glass cables associated with polypropylene	Polyester
Unit weight (g/m²)	340	268.1
Gris size (mm × mm)	25×25	40×40
Content of bitumen (%)	Uncoated	> 60

2.2. Testing programs

The experimental study consists of evaluating, the flexural strength and the modulus of rupture, using seven different prismatic beams (305×90×75 mm): standard beam (control), beam with emulsion1 and beam with emulsion2, beam reinforced by geogrid1 with emulsion1, beam reinforced by geogrid1 with emulsion2, beam reinforced by geogrid2 with emulsion1 and beam reinforced by geogrid2 with emulsion2. For each test, two specimens were tested and the average values strength and modulus of ruptura are reported. The deflection was measured with a linear variable displacement transducer (LVDT), and the load-displacement curves were plotted.

Three point vending tests were also conducted on eight pre-cracked asphalt concrete slabs of 500×180×100 mm, with the insertion of emulsions and geogrids: standard slab not pre-cracked (reference), pre-cracked-reference slab, pre-cracked slab with emulsion1, pre-cracked slab with emulsion2, pre-cracked slab with emulsion1 and geogrid1, pre-cracked slab with emulsion2 and geogrid1, pre-cracked slab with emulsion2 and geogrid1 and

pre-cracked slab with emulsion2 and geogrid2. The objective of this second serie of tests is to evaluate the crack propagation on the behaviour of each emulsion and geogrid reinforced bituminous slab (30, 31).

2.3. Preparation of the specimens

A total of 30 (thirty) specimens were made with the same composition of bituminous concrete. These specimens are divided into two categories: the first category, with a number of 14 (fourteen) prismatic beams in the form of rectangular shaped slabs (305×90×75) mm, composed of two layers of asphalt concrete, cationic emulsion (E1 or E2) and geogrids (G1 or G2). Table 2 shows the details and identification of the manufactured slabs tested under three-point bending test with a span of 240 mm where the flexural strength and modulus of ruptura were determined. Deflection was measured using a linear variable displacement transducer (LVDT), in accordance with ASTM E2309 (32). All tests were were conducted at 20°C, under displacement control at a constant speed of 50.8 mm/min.

The slabs of this first category represent a simulation of the repair of a deteriorated asphalt layer and recharged by a top layer with emulsion bonding and geogrid insertion. In effect, the lower layer simulated an existing deteriorated asphalt layer and the upper layer represented the reinforcement layer (overlay). The first step in the manufacture of the slabs was to produce a 50 mm high asphalt concrete layer in an appropriately sized mould and to compact it using the rolling compaction procedure in accordance with NF-EN 12697-33 (33).

The second category is composed of 16 pre-cracked slab specimens of dimensions (500×180×100 mm), made with a concrete-asphalt mixture, prepared in accordance with European standards (EN 12697-35) (34). These slabs are composed of layers of asphalt concrete, cationic emulsion (E1 or E2) and geogrids (G1 or G2). Table 3 shows the details and identification of these slabs.

The calculated amount of mixture was poured into preheated moulds of dimensions (500×180×100 mm) and compacted in the laboratory using the roller plate compactor in accordance with the above-mentioned standard (EN 12697-33).

The production of the double-layer slabs was carried out in several stages. In the first stage, the bottom layer was compacted to a thickness of 50 mm, which resulted in an air void content of approximately 5%. After cooling the slab for 4 hours in the laboratory, the bituminous emulsion was spread at the interface and left for 1 hour in the air to evaporate. Then the geogrid was carefully placed and a 50 mm top bituminous layer was applied and compacted (Figure 4a). Compaction was applied until an air void content of

TABLE 2. Details of the prismatic beams tested.

Identification	Size (mm)	Nomination	Test
Reference	(305×90×75)	R	3- point bending
With emulsion 1	(305×90×75)	E1	3- point bending
With emulsion 2	(305×90×75)	E2	3- point bending
Emulsion1 + Geogrid1	(305×90×75)	E1G1	3- point bending
Emulsion2 + Geogrid1	(305×90×75)	E2G1	3- point bending
Emulsion1 + Geogrid2	(305×90×75)	E1G2	3- point bending
Emulsion2 + Geogrid2	(305×90×75)	E2G2	3-point bending

TABLE 3. Details of pre-cracked beams of the 2nd category.

Identification	Size (mm)	Nomination	Test
Reference (uncracked)	(500×180×100)	RR	3- point bending
Reference (pre-cracked)	(500×180×100)	PRR	3- point bending
Pre-cracked with emulsion1	(500×180×100)	PE1	3- point bending
Pre-cracked with emulsion2	(500×180×100)	PE2	3- point bending
Pre-cracked with emulsion1 + geogrid1	(500×180×100)	PE1G1	3- point bending
Pre-cracked with emulsion2 + geogrid1	(500×180×100)	PE2G1	3- point bending
Pre-cracked with emulsion1 + geogrid2	(500×180×100)	PE1G2	3-point bending
Pre-cracked with emulsion2 + geogrid2	(500×180×100)	PE2G2	3- point bending

approximately 5% was achieved. The determination of the latter was done according to NF EN 12697-8 (35). Finally, the direction of compaction was marked on the surface of the slab in order to carry out the tests in the correct direction of traffic.

In order to simulate a flexible pavement (road or airfield), with matching cracks, a 40 mm notch was made at the base of the manufactured slab (10 mm below the geogrid) by sawing to impose the location of the crack initiation (Figure 4a). Thus, during the test, the crack propagation starts at the location of the pre-crack. In order to perfectly visualise the crack path, a layer of plaster was spread over the central area of the samples. The objective of this second category of
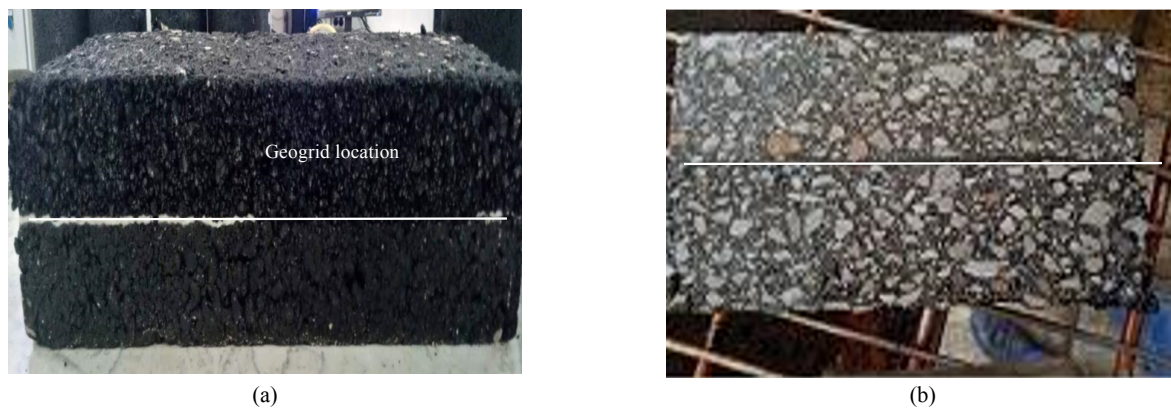

(a)

(b)

FIGURE 4. a) Test specimen with geogrid location, b) Test specimen with fracture crack.

specimens is to study the effect of crack propagation on the behaviour of a slab reinforced (Figure 4b), simultaneously, with a geogrid layer and the type of emulsion chosen (36).

3. HEAVY WEIGHT DEFLECTOMETER TESTS

Non-destructive in situ tests, were carried out with a heavy duty deflectometer (HWD) in the main directions (longitudinal and transversal) of the runway of the national aerodrome of Ouargla (800 km south-east of Algiers), before and after its reinforcement by the application of a tack coat on the degraded layer and the insertion of a geogrid. Emulsion (E2) and non-woven geogrid were used, given their good performance during the laboratory tests.

3.1. Description of the falling weight deflectometer

This is a non-destructive test device designed to reproduce, by means of an impact on a disc in contact with the road surface, the load corresponding to half an axle of a truck travelling at approximately 80 km/h and to measure, at the same time, the deflections generated on the surface. This test offers the possibility to vary the intensity of the applied load according to the structural stiffness observed in situ (37). HWD loads, designed for roadways and airports, are generally between 20 and 75 kN. This device could be used to make relative comparisons of pavements based on deflection indices and to determine the structural capacity of pavements and the modulus of elasticity of material layers by back-calculation. HWD can also be used to calculate deformations and stresses in pavements, detection of voids under slabs and as a tool for pavement quality control during construction.

HWD is used for deflection testing on flexible or rigid pavements on airport runways using additional loads where the total load can be up to 250 kN (38).

3.2. Ouargla runway case study

The case study concerns the main runway (02/20) of an airfield that was commissioned in 1951 and consists of two runways of 3000 × 45 m each. Its pavement is composed of several sub-layers (Figure 5) and this infrastructure has been the subject of several reinforcement and modernisation works since it was commissioned. This runway is operated by various aircraft and the critical aircraft criticized for the study is a Boeing 737-800 (39).

The procedure of reinforcement by insertion of the emulsion layer and geogrid sheet was as follows:
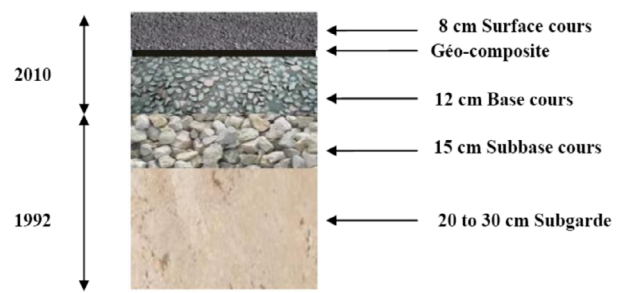- Scarification of 60 mm of the existing load-bearing asphalt concrete layer;

FIGURE 5. Composition of the pavement layers.

- Sealing of exposed cracks;
- Application of an adherent asphalt layer to the scarified surface;
- Laying the geogrid layer on the central part of the runway, i.e. 2400 × 30 meters;
- crossing wide-tyred trucks over the geogrid layer to remove the air trapped underneath;
- Careful application of the asphalt concrete layers to the recommended thickness;
- Finishing work.

The geogrid used for the reinforcement of the main runway 02/20 and ancillary structures is a non-woven geocomposite composed of continuous polypropylene filaments combined with glass fiber cables, known as PGM-G 50x50 (Figure 6). This non-woven geogrid composed of continuous glass filaments and polypropylene fibers type of geogrid was used because of its superior properties. These geogrids were different than those used in the laboratory tests because of their unavailability from the manufacturer during the laboratory tests (40).

FIGURE 6. Geogrid application on runway.

Deflection measurements in the longitudinal direction were carried out by preforming six measurement profiles located at 3.5 m, 6.5 m and 12 m on either side of the main runway axis (Figure 7). The measurements were carried out before the reinforcement of the runway with geogrids (in 2009) and then after the reinforcement, i.e. seven years later (in 2017), in order to monitor its behaviour over time. A comparison between the two measurements is made to assess the effect of the geogrid reinforcement on the values

of the deflections and stresses of the running surface (bituminous concrete). The comparison between the state of the runway, before and after its reinforcement, allows the contribution of the asphalt layers reinforced by the geogrid to the bearing capacity of the lower layers to be estimated.
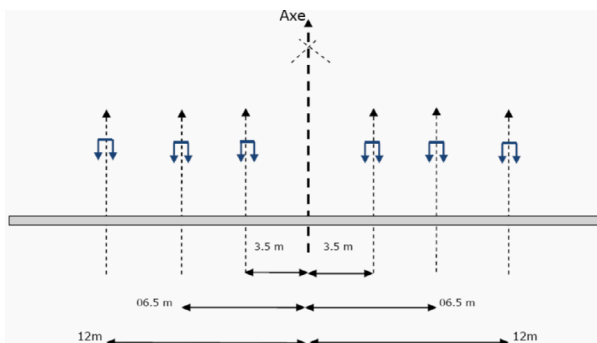

FIGURE 7. Layout of profiles on either side of the axis.

4. RESULTS AND DISCUSSION

4.1 Flexural strength and modulus of rupture

The first results obtained during the experimental investigation, in the laboratory, are presented in Figure 8, observing the evolution of the flexural strength. These are -the load-displacement curves of the different prismatic beams tested are given in Figure 8. The maximum load is determined at full crack propagation, prior to total failure of the specimen. In all the tests carried out, the specimens failed ductilely, without tearing or disintegration of the applied geogrid. For the control beam, referred to as "R", the maximum load value was 15.37 kN, for a mid-span displacement of 0.223 mm. The use of the emulsion layer type 2 (E2) is more effective than the one used for the emulsion E1, due to the higher percentage of 69% compared to 65%. The maximum load value is 16.83 kN (gain of 9.50%) for E2, compared to 16.27 kN (gain of 5.86%) for E1. The use of an emulsion layer seems to give a non-negligible gain in flexural strength (41). The insertion of the geogrid, with the emulsion layer at the interface, avoids the provocation of the disbonding effect between the layers (42) and ensures an appreciable cohesion and gain for the pavement (the beam in our case). Type 1 of the geogrid with E1 emulsion (E1G1 beam), gives a value of 21.17 kN (a gain of 37.74%), compared to the value of 22.38 (G1 geogrid + E2 emulsion), therefore a gain of 45.61%. The E2 emulsion, with the G1 geogrid (E2G1), gave a value of 22.53 kN (gain of 46.58%), compared to the value of 23.08 kN (a gain of 50.16%). These results show that it is more favorable to apply geogrid type 2 (or any equivalent type), with the tack coat (E2 emulsion) for any reinforcement as the gain is more than 50%.
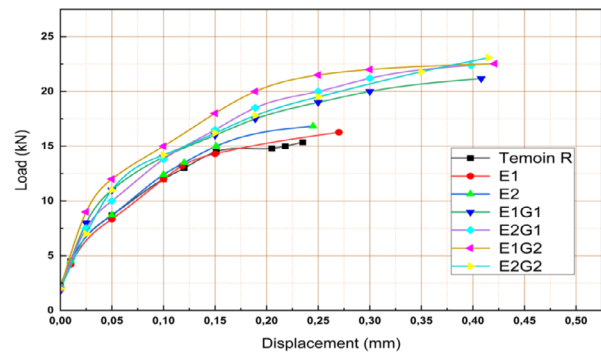

FIGURE 8. Force-displacement diagrams for tested beams.

For the deflections (displacements at mid-span of the tested beam), the above curves shows that the maximum displacement of the control beam (R) is of the order of 0.353 mm, whereas for the G2 reinforcement and E1 emulsion, it is of the order of 0.415 mm, i.e. an increase of 19.26%, opposing only 0.415 mm (gain of 17.56%) for the E2G2 beam and 0.398 mm (gain of 12.75%), for the E2G1 beam. Concerning the emulsions applied alone at the interface, which ensure good bonding (adhesion), reductions in deflections were observed (0.270 mm for E1 and 0.245 mm for E2), i.e. significant gains of the order of 23.51% (emulsion E1) and 30.59% for emulsion E2 respectively. These tests also showed the importance of the emulsion for the bonding of asphalt concrete layers, where the mechanical performance is improved. The gain in mechanical performance is more important when geogrids are used as reinforcement by the use of emulsion, where the gain can reach 50% for the applied force and 31% for the displacements. Consequently, the increase in mechanical performance is closely related to the increase in adhesion between the two bituminous layers and between the bitumen and the geogrid. The comparison between the two types of geogrids used shows that the type 1 geogrid gave lower performance due to its insufficient resistance to lateral movements. For the evolution of the modulus of rupture (MOR), which is defined as the maximum stress that any rectangular prismatic beam can withstand when subjected to bending and which allows the evaluation of progressive damage, generally related to cracking (43), Table 4, gives the values found during the different tests of the specimens used. These results shows that the insertion of the geogrid sheet improves the modulus of rupture (MOR) by 8.74% for the beam (E2G2), 7.32% for the beam (E1G2), 4.47% for the beam (E2G1) and 4.07 for the beam (E1G1). The beams with emulsions E1 or E2, do not seem to give any gain in modulus of rupture (MOR), which proves that the emulsions, in spite of the adhesion they provided, do not influence the stress at rupture.‑

TABLE 4. Modulus of rupture evolution for the tested beams.

Identification	Modulus of rupture (MPa)	Gap (%)
Reference (R)	4.92	-
With emulsion1 (E1)	5.12	- 4.07
With emulsion2 (E2)	5.24	-6.50
Emulsion1 + Geogrid1 (E1G1)	4.72	4.04
Emulsion2 + Geogrid1(E2G1)	4.70	4.47
Emulsion1 + Geogrid2 (E1G2)	4.56	7.32
Emulsion2 + Geogrid2 (E2G2)	4.49	8.74

4.2. Evolution of crack propagation

The three points bending test was chosen to evaluate the perfromance of the pre-cracked slabs because it produces the maximum bending moment at the middle of the slabs. Figure 9 shows the different load-displacement curves obtained for the slabs tested.
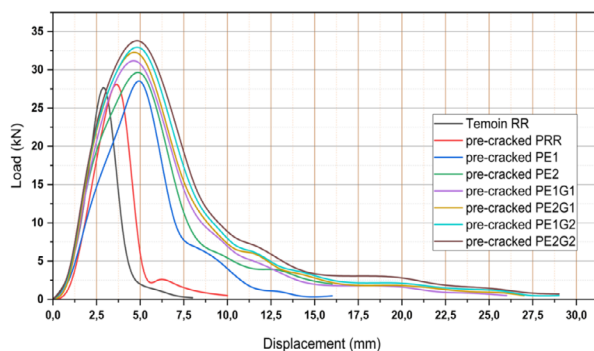

FIGURE 9. Load-deflection curves for precast slab bending tests.

The load-deflection curves show that for each slab tested, the maximum load (Pmax) is the failure one, with a clear advantage for geogrid-reinforced slabs bonded with emulsion layers. The area under each curve is composed of two zones: the zone under the curve up to the flexural strength (Pmax), which represents the crack initiation energy (Ei), while the zone under the curve from Pmax to the failure of the specimen is the pre-crack propagation energy (called Eup) and the curve between Pmax and the failure of the slab, which is the crack propagation energy (called Ep). It is noted that no cracks occurred or appeared (neither ordinary, nor of contiuation of the pre-crack) in the specimens, before the maximum load Pmax (44).

As all our specimens (slabs) are made of two layers, the energy (Ep) is the sum of the energy necessary for propagation in the lower layer (Einf) and the energy necessary for propagation in the upper layer (Esup). The values of Ei and Ep are calculated by the areas under each curve by discriminating the curves. It was observed that the cracks started to propagate from the notch tip (pre-crack), location of the stress's highest concentration and then upwards in the direction of the applied load, perpendicular to the maximum principal tension (45). It has been reported that in the case of reinforced pavements, the reinforcement mainly affects the crack propagation in the top layer (asphalt concrete wearing course) (46). Based on the results obtained, it can be seen from Figure 9, that the unreinforced and non-pre-cracked slab (RR) has a higher value of flexural strength (Pmax) (27.45 kN) than the unreinforced and pre-cracked slab (PRR) (24 kN) and this is due to the higher failure energy, as a result of not facilitating crack initiation (no presence of notch). The introduction of the emulsion layers ensured an adequate bond between the interface of the slab and the double layer (47). Values of the order of 28.5 kN for the pre-cracked slab with emulsion E1 (PE1) and 29.2 kN for the pre-cracked slab with emulsion E2 (PE2) were obtained, confirming the absence of disabonding at the interface.

The insertion of the geogrid sheet seems to give a very appreciable gain, with Pmax values for the slabs reinforced respectively by the type 1 geogrid and the type 2 geogrid, namely 30.2 kN (slab PEIGI), 31.4 kN (slab PE2G1), against the values of 32.5 kN (slab) PE1G2 and 33.4 kN (slab PE2G2 . The gain values are 21.70% (slab PE2G2), 18.40% (PE1G2 slab), 14.39% (slab PE2G1), 10.02% (slab PE1G1). The emulsions gave insignificant gains for Pmax, with a value of 6.38% (slab PE2) and 3.83% (slab PE1). The quantification of the contribution of the geogrid in the crack propagation phase is given, first, by the value of the crack propagation energy (EP), summing its value before and after the failure phase (Table 5). The coefficient of performance (k), defined as the ratio of the propagation energy of the unreinforced and pre-cracked slab (PRR) after failure, to the propagation energy of the reinforced and pre-cracked slab, is detailed in the Table below.

The results found, shows that the coefficient of performance (k), for the specimens tested in the laboratory and calculated for maximum deflection at mid-span, is influenced by the mode and type of reinforcement. It can be observed that, in addition to the bonding emulsions, all geogrids significantly increase the crack propagation (coefficient k) and significantly increase the crack propagation energy (Eup). Indeed, if the emulsions increase by almost 83% (E1 emulsion) and 143% (E2 emulsion), the geogrids surpass these Figures by far, with a percentage varying from 149% (PE1G1 slab), 157% (PE2G1 slab), 173% (PE1G2 slab) and 237% (PE2G2 slab).

These results show that the geogrid reinforcement (G2) with emulsion bonding (E2) performs best and delays the crack propagation in the notch above the

TABLE 5. Evolution of the fracture energy and the coefficient (k).

Identification	Energy before faillure (Ei) (kN-mm)	Energy after failure (Eup) (kN-mm)	Coefficient (k)
Reference (RR)	34.31	41.81	-
Pre-cracked (PRR)	39.00	48.25	-
Pre-cracked (PE1)	71.25	88.13	2.26
Pre-cracked (PE2)	75.92	117.17	3.00
Pre-cracked (PE1G1)	78.52	119.77	3.07
Pre-cracked (PE2G1)	81.64	123.89	3.18
Pre-cracked (PE1G2)	84.50	131.72	3.38
Pre-cracked (PE2G1)	86.84	162.34	4.16

reinforcement. The coefficient of performance (k) varies from a value of 2.26 (E1 emulsion) to a value of 4.16 (G2 reinforced slab and E2 emulsion), i.e. a difference of 84%, clearly indicates, that the service life of the reinforced asphalt pavement increases, by delaying the upward cracking and the reflection crack.

4.3. Behaviour of the track tested with HWD

4.3.1. Deflections and stresses at geophone positions

The determination of the values of deflections (displacements) at the different positions of the geophones (called D1 to D9), located in the right part of the longitudinal axis of the tested runway, before and after its reinforcement with geogrids, is shown in Figures 10 and 11. The evaluation was made by comparing the average values of the maximum deflection (in μm), recorded at each position of the geophone, on the one hand, and by reading the measured stress (in kPa), on the other. These values are given simultaneously in the record by the HWD test (48). The values of deflection and stress are given by the central geophone D1, which are 728 μm and 2610 kPa (before reinforcement) and 786 μm and 2975 kPa (after reinforcement), respectively. This means an average reduction of 7.89% for the deflection of the wearing course and an average increase of 13.98% for the stress. The reduction in deflection values reflects the contribution of the reinforcement, together with the tack coat, to the bearing capacity of the pavement of the reinforced runway.

4.3.2. Evolution of the elastic modulus

The interpretation of the data generated by the HWD test is based on inverse analysis processes. In fact, the data of the falling weight technique, combined with the thickness of the pavement body
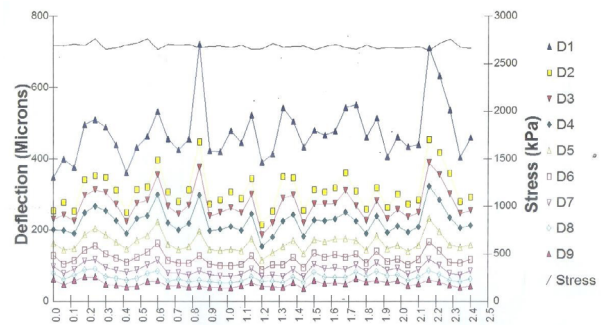

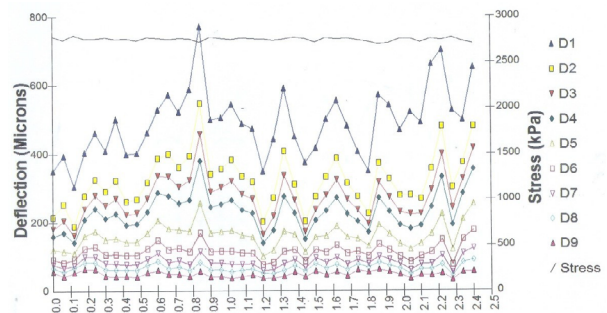FIGURE 10. Deflection and stress before reinforcement with geogrid of the runway.

FIGURE 11. Deflection after reinforcement with geogrid of the runway.

layers, provide information on the evolution of the Young's modulus (elastic modulus) of each layer of the structure along the profile of the flexible track studied (49). This information can also be used to estimate the service life of the structure and any repairs required. The variation of the modulus of elasticity of the pavement of the emulsion-reinforced runway and the geogrid insertion is given in Figure 12 (before reinforcement) and Figure 13 (after reinforcement), respectively. Before reinforcement and with the degraded state of the runway, the average modulus of elasticity E1 of the bituminous

layer, varies between 2869 MPa and 3113 MPa, with an overall average equal to 2979 MPa. The second measurements were carried out seven years after rehabilitation (reinforcement of the runway) gave values ranging from 4881 MPa to 5895 MPa, with an overall average equal to 5538 MPa.

These values show that the mechanical behaviour of the runway (with interface emulsion) is improved by 86% in the presence of a geogrid and that the life of the runway pavement can be extended (50).
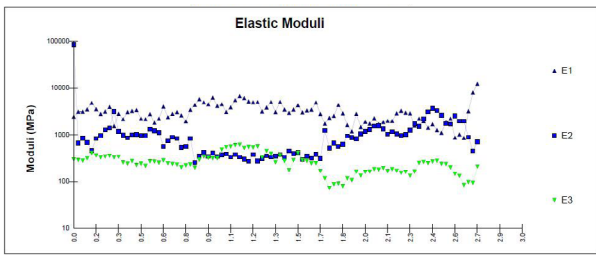

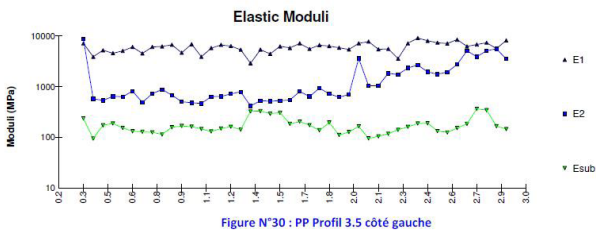**Figure 12.** Elastic modulus before geogrid reinforcement of the runway.

Figure 13. Elastic modulus after geogrid reinforcement of the runway.

4.3.3. Comparison and discussion of values

The recorded average deflections, elastic modulus and stresses before and after reinforcement, in the different positions of the tested runway width, are represented in Figures 14, 15 and 16. These are the values measured for geophone D1 (the most unfavourable). A considerable improvement in the value of the base course modulus for geogrid-reinforced pavements compared to the unreinforced section is obtained. it can also be seen that the correlation between the stiffness of the geogrid type used and the thickness of the base course of the reinforced pavement is satisfactory (51). From a practical point of view, the results obtained can be used to improve the design catalogue of flexible pavements, in particular for those reinforced with geosynthetics (such as geogrids), for combinations of traffic loads and base course CBR values.
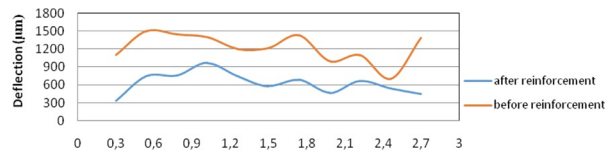

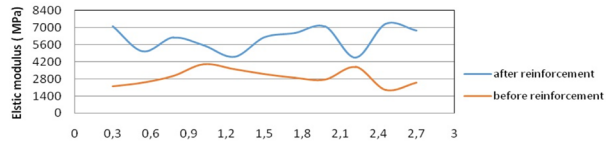**Figure 14.** Deflections at geophone D1 before and after strengthening.

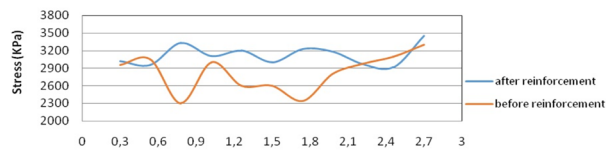**Figure 15.** Elastic modulus E1 before and after runway strengthening.

Figure 16. Stresses before and after strengthening of the runway pavement.

4. NUMERICAL ANALYSIS

In order to calibrate the results, found for the prismatic beams in the laboratory, a three-dimensional numerical modeling (x-y-z), using the finite element method (FE), was developed using a commercial software, which is based on the input of the geometrical and mechanical characteristics of the experimental beam, of the bonding emulsion and of the geogrid used The geometry, support conditions and loads are similar to those of the developed experimental work (52). Meshing and convergence analyses were performed by testing the different models.

Four types of elements were chosen to model the cross-section of the tested specimen (beam). All these elements were expressed in the adapted software, according to the criteria of Mohr-Coulomb (53). The elements, of the asphalt concrete, were chosen as isotropic block elements, while the elements chosen for the geogrid, and the bonding emulsion, were one-dimensional linear elastic block elements. The finite element model was validated by comparison with the results of the laboratory experimental tests. Table 6 shows all the mechanical characteristics of the materials used in the modeling, As the dimensions of the prismatic beam are involved and in order to save computational time, mesh and convergence analyses have been performed by testing the different models.

Typical stresses and displacements, before and after reinforcement and along the main loading axis (static), are shown in Figures 17a to 17g. The values obtained indicate that the geogrids, whatever their results in a reduction in vertical stresses when placed at the depth of the pavement (at the interface). The

TABLE 6. Material characteristics used for the beam analysis.

Material	Young's modulus (MPa))	Poisson's ratio	Thiclness (mm)
Asphalt concrete 1st layer	4000	0.25	50.0
Asphalt concrete 2nd layer	7000	0.25	23.0
Asphalt concrete 2nd layer E1	7500	0.25	51.0
Asphalt concrete 2nd layer E2	8000	0.25	51.0
Emulsion E1 + Geogrid G1	750	0.30	2.0
Emulsion E2 + Geogrid G1	800	0.30	2.0
Emulsion E1 + Geogrid G2	850	0.30	2.0
Emulsion E2 + Geogrid G2	900	0.30	2.0

tack coat (E1 or E2), created good adhesion between the two sub-layers (two-layer) and ensured that they did not delaminate or slip. The simultaneous combination (emulsion + geogrid) gave an appreciable gain in stress, thus the applied load of failure.

The highest values found for the stress of the control beam "R" (without reinforcement) is in the order of 40.506 MPa (Figure 17a), while the beam with emulsions E1 and E2, gave, respectively, maximum values of 48.506 MPa (Figure 17b) and 52.728 MPa (Figure 17c). The emulsions gave gains ranging from 19.75% to 30.17%. For the simultaneous insertion of the emulsion and the geogrid, values of 53.428 MPa (beam E1G1), a gain of 31. 90%, 71.407 MPa (beam E2G1), i.e. a gain of 76.29%, 71.995 MPa (beam E1G2), i.e. a gain of 77.74% and finally 73.92 MPa (beam E2G2), i.e. a gain of 82.49%. These results confirm the conclusions of previous similar studies, such as those of: Correia (54) and Rahman (55), who studied the flexibility of flexible pavements using finite element (FE) modelling.
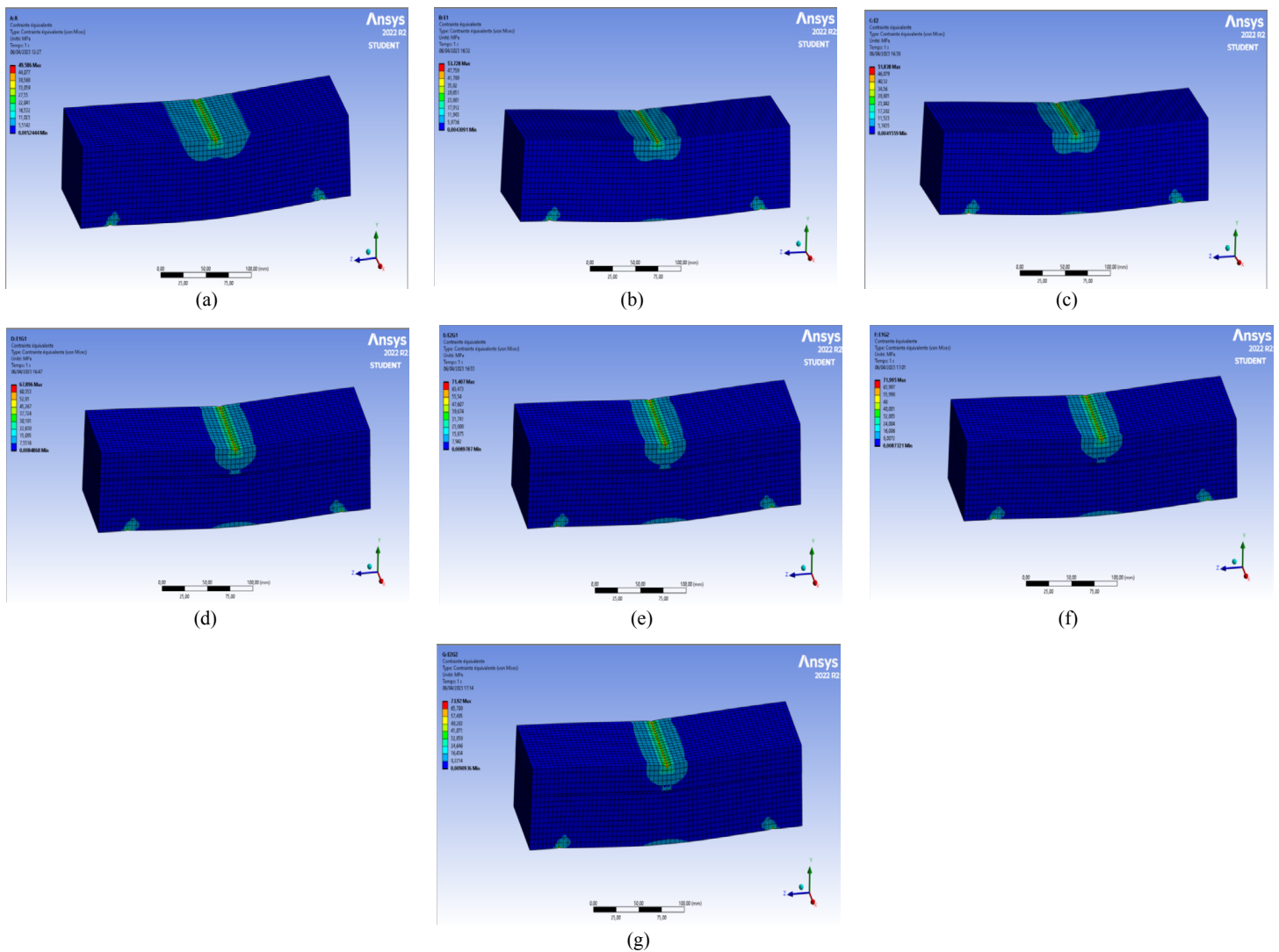

FIGURE 17. a) Stress status of beam R, b) Stress status of beam E1, c) Stressed state of beam E2. d) Stress state of beam E1G1, e) Stressed state of beam E2G1, f) Stressed state of beam E1G2, g) Stress status of beam E2G2.
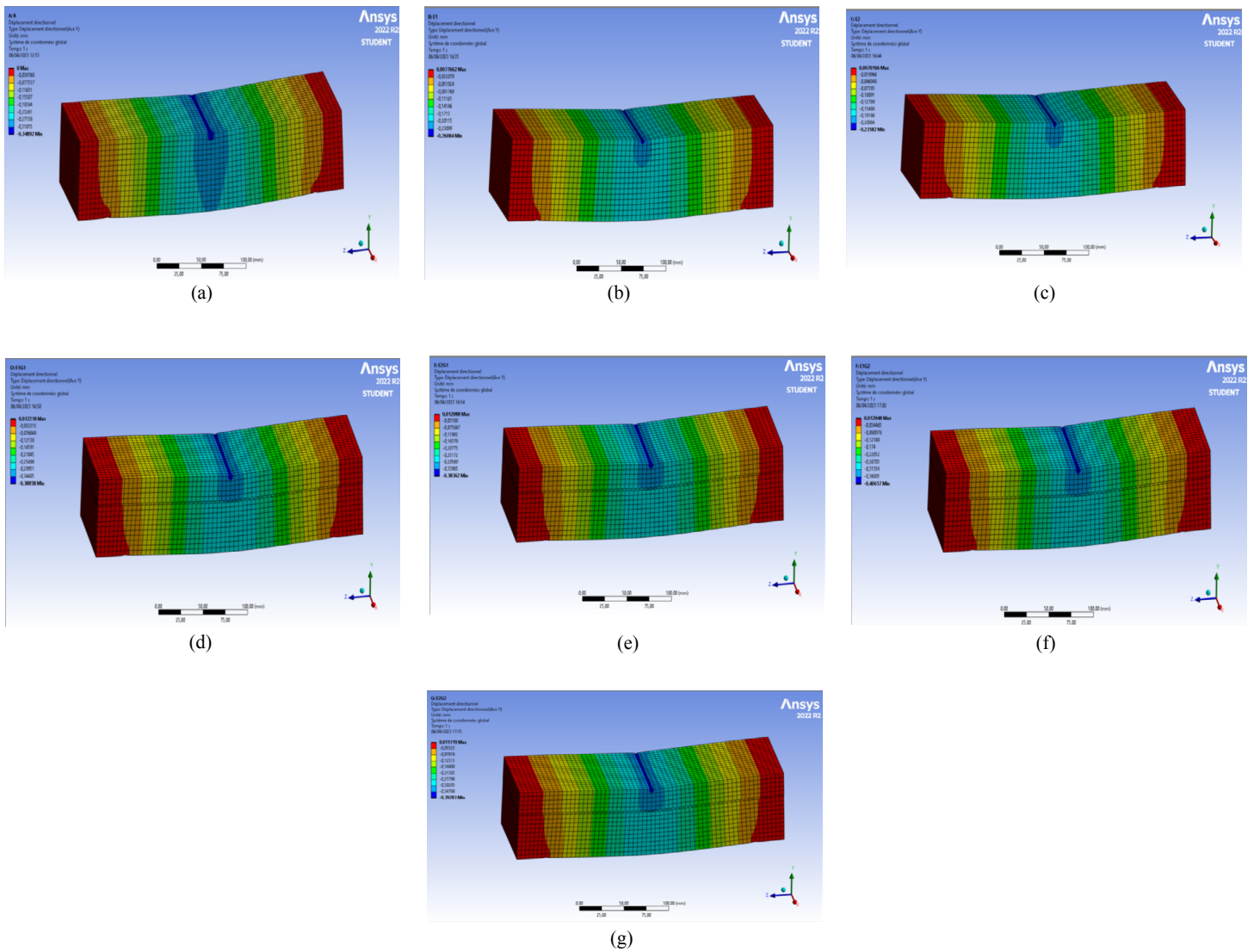
(a)

(b)

(c)

(d)

(e)

(f)

(g)

FIGURE 18. a) Displacement status of beam R, b) Displacement status of beam E1, c) Displacement status of beam E2, d) Displacement status of beam E1G1, e) Displacement status of beam E2G1, f) Displacement status of beam E1G2, g) Displacement status of beam E2G2.

TABLE 7. Comparative values experimental – numerical.

Identificatn	Stress (MPa)			Deflecion (mm)		
	Experimental	FEM	Gap (%)	Experimental	FEM	Gap (%)
Beam R	41.52	40.506	2.45	0.353	0.349	1.13
Beam E1	54.24	52.728	2.78	0.270	0.261	3.34
Beam E2	50.26	48.506	3.49	0.245	0.236	3.67
Beam E1G1	54.27	53.428	1.55	0.408	0.388	4.90
Beam E2G1	73.71	71.407	3.12	0.398	0.384	3.52
Beam E1G2	74.08	71.995	2.81	0.421	0.406	3.56
Beam E2G2	75.68	73.920	2.36	0.415	0.393	5.30

Regarding the deflection values found by the numerical modeling, it can be seen that the maximum displacement (in compression) at mid-span for the control beam (R) has a value of 0.349 mm (Figure 18a). For the beams with emulsion in the bilayers, values of 0.261 mm (Figure 18b) were found for the beam with emulsion E1 and 0.236 mm (Figure 18c), for the beam with emulsion E2. Gains of 25.21% for E1 and 32.38% for E2.

For the prismatic beams with emulsion and geogrid reinforcement (Figures: 18c, 18d, 18e, 18f and 18g), the values of the deflections are higher than the R-beam or the beams with emulsion (E1 or E2). This is due to the fact that the geogrid, as a result of the role it plays, slightly increases the deformation, which is by virtue to the higher stresses values (load) at failure. The beam strengthened by the geogrid G1 and emulsion E1 (E1G1), gave a value of 0.388 mm, i.e. an increase of 11.74%, similarly for the beam (E2G1), a value of 0.384 mm was found, i.e. an increase of 10.03%. The beams reinforced with the G2 geogrid have values of 0.408 mm (E1 emulsion) and 0.393mm (E2 emulsion) respectively, an increase of 16.33% and 12.61%.

The comparison made between the experimental and numerical values found, for the case of the prismatic beam (with emulsion and reinforcement) showed that the difference between the predicted numerical values and the measured experimental results did not exceed, 5% (Table 7), which could be improved if a non-linear behaviour of the materials is used. The stresses obtained from the numerical analysis gave comparable values to those of the laboratory tets, with differences ranging from 1.55% to 3.89%, confirming that the chosen model is acceptable. The differences in deflection values range from 1.13% to 5.30 %. It can also be concluded from both analyses (experimental and numerical analysis) that geogrids with good emulsion adhesion, regardless of their type, improve the longevity of flexible pavements increase their bearing capacity (56).

5. CONCLUSIONS

The experimental test results of two categories of samples, simulating a degraded flexible pavement loaded to failure and pre-cracked asphalt slabs statically loaded to crack propagation from the notch as well as the in-situ pseudo-dynamic evaluation on a runway and the finite element modeling led to the following conclusions:
- The geogrid, in addition to its role as a separator, can play the role of reinforcement and becomes more efficient by applying bonding emulsions at the interfaces of the bilayers.
- The geogrids increased the crack propagation energy in the layer above the reinforcement by two to five times:
- In the presence of emulsion binders, the bond between the asphalt layers does not deteriorate (debonding effect), which results in a higher bond strength for the two layers;
- The three-point bending tests showed ductile behaviour of the geogrid-reinforced specimens and no tearing or disintegration of the geogrid was observed;
- The stresses are reduced by up to 50% and the displacement is redued by 20% when geogrids with a layer of emulsion at the interface are used.
- For pre-cracked slabs, the insertion of a geogrid layer with cathodic emulsion improves the modulus of rupture (MOR) by nearly 10% and the damping coefficient (k) is of the order of 2 to 5, which increases the service life of the reinforced asphalt pavement, by delaying upward cracking and reflection cracking;
- The pseudo-dynamic HWD test was able to provide insights into the behaviour of the runway before and after reinforcement and confirmed that the goesynthetics reduced the stiffness of the asphalt layers compared to the unreinforced pavement, which corroborates the laboratory results;
- The numerical analysis proved that the chosen model is in perfect harmony with the reality of the tested samples. Variations in deviation of 2 to 5% are still excellent and this deviation can be reduced by using a non-linear behaviour of the materials used (bituminous concrete, bitumen layer, emulsion layer, geogrid, etc.);
- It is recommended that further work is performed The generalisation of this type of work on other real size flexible or rigid airfield runway or road pavements.

Authorship contribution statement

Rabia Bazine: Investigation, Data curation, Writing, original draft.
Mouloud Abdessemed: Conceptualization, Data curation, Supervision, Funding acquisition, Validation, Writing, review & editing.
Said Kenai: Conceptualization, Data curation, Writing, review & editing.
Noureddine Ouadah: Modeling, Writing, original draft.

The authors of this article declare that they have no financial, professional or personal conflicts of interest that could have inappropriately influenced this work.

REFERENCES

1. National Economic and Social Council (CNES). 2005. The development of road infrastructure: Needs for economical choice and better transport security in French. 25th pleinary session CNES Publication Algiers Algeria.
2. Public Transport Ministry (MTPT). Infrastructure General Directorate. 2019. Evaluation of Algerian road network in French.; Algiers Algeria.
3. Susanna A, Crispino M, Giustozzi F, Toraldo E. 2017. Deterioration trends of asphalt pavement friction and roughness from medium-term surveys on major Italian roads; Int. J. Pavement Res. Technol. 10(5):421-433. http://doi.org/10.1016/j.ijprt.2017.07.002.
4. Abu El-Maaty AE. 2017. Temperature change implications for flexible pavement performance and life. Int. J. Transp. Eng. Technol. 3(1):1-11. http://doi.org/10.11648/j.ijtet.20170301.11.
5. Chen Y, Wang H, Xu S, You Z. 2020. High modulus asphalt concrete: A state-of-the-art review. Constr. Build. Mater. 237:117653. http://doi.org/10.1016/j.conbuildmat.2019.117653.
6. Lacalle-Jiménez HI, Edwards JP, Thom NH. 2017. Analysis of stiffness and fatigue resistance of cold recycled asphalt mixtures manufactured with foamed bitumen for their application to airfield pavement design. Mater. Construcc. 67(327):e127. https://doi.org/10.3989/mc.2017.04616.
7. Perkins SW, Ismeik M. 1997. A synthesis and evaluation of geosynthetic- reinforced base layers in flexible pavements-Part I. Geosynth. Int. 4(6):549-604. https://doi.org/10.1680/gein.4.0106.
8. Mirzapour Mounes S, Rehan Karim M, Khodaii A, Hadi Almasi H. 2014. Improving rutting resistance of pavement structures using geosynthetics- An overview. Hindawi Publishing Corporation. 2014:764218. http://doi.org/10.1155/2014/764218.
9. Indraratna B, Khabbaz H, Salim W. 2012. A laboratory study on improvement of railway ballast using geosynthetics. Geotech. Eng. Transp. Projects. 617-626. https://doi.org/10.1061/40744154.48.
10. Giroud JP, Ah-Line C, Bonaparte R. 1984. Design of unpaved roads and trafficked areas with geogrids- polymer grid reinforcement A conference sponsored by SERC and Netlon Ltd. Thomas Telford London England 116-127.
11. Anderson P, Killeavy M. 1989. Geotextiles and Geogrids - Cost effective alternate materials for pavement design and construction. Proceedings of Geosynthetics '89 IFAI. Sand Diego California USA. 2:353-360.
12. Abdessemed M, Kenai S, Bali A. 2015. Experimental and numerical analysis of the behavior of an airport pavement reinforced by geogrids. Constr. Build. Mater. 94:547–554. https://doi.org/10.1016/j.conbuildmat.2015.07.037.
13. Jasim AF, Fattah MY, Al-Saadi IF,Abbas AS. 2021. Geogrid reinforcement optimal location under different tire contact stress assumptions. Int. J. Pavement Res. Technol. 14:357–365. https://doi.org/10.1007/s42947-020-0145-6.
14. Al-Qadi IL, Dessouky SH. Tutumluer E. 2008. Geogrid in flexible pavements: validated mechanism. Transportation Research Record: Transp. Res. Rec.: J. Transp. Res. Board. 2042 (1). https://doi.org/10.3141/2045-12.
15. Abdessemed M, Khengaoui S, Kenai S. 2021. Diagnostic d'une infrastructure linéaire rigide - analyse expérimentale après renforcement par geogrilles. Acad. J. Civ. Eng. 38(2):144-148. https://doi.org/10.26168/10.26168/ajce.38.2.33.
16. Austin RA, Gilchrist AJT. 1996. Enhanced performance of asphalt pavements using geocomposites. Geotext. Geomembr. 14(3-4):175-186. https://doi.org/10.1016/0266-114496.00007-6.
17. Alimohammadi H. Zheng J, Schaefer VR, Siekmeier J, Velasquez R. 2021. Evaluation of geogrid reinforcement of flexible pavement performance: A review of large-scale laboratory studies. Transp. Geotech. 27(100471). https://doi.org/10.1016/j.trgeo.2020.100471.
18. Abdessemed M, Bazzine R, Kenai S. (2022). Application of the synthetics geo-composites in the arid zones for rehabilitation of the flexible pavements road experimental analysis. In: Di Benedetto H, Baaj H, Chailleux E, Tebaldi G, Sauzéat C, Mangiafico S. (eds) Proceedings of the RILEM International Symposium on Bituminous Materials. ISBM 2020. RILEM Bookseries, Springer, Cham. 27:279–284. https://doi.org/10.1007/978-3-030-46455-4_35.
19. Freire RA, Di Benedetto H, Sauzéat C, Pouget S, Lesueur D. 2021. Crack propagation analysis in bituminous mixtures reinforced by different types of geogrids using digital image correlation. Constr. Build. Mater. 303:124522. https://doi.org/10.1016/j.conbuildmat.2021.124522.
20. Afnor Editions Normes NF EN 13108-1. 2008. Mélanges bitumineux - spécifications des matériaux - Partie 1: enrobés bitumineux 53 pages. Indice de classement: P 98-819-1, ICS: 93.080.20. Lavoisier France.
21. Total France Direction Bitumes. 2006. Caractéristiques techniques AZALT- Bitumes routiers de la norme NF EN 12591. Retrieved from https://services.totalenergies.fr/pro/produits-services/bitumes.
22. Afnor Editions Normes NF EN 13285. 2018. Graves non traitées – Spécifications Normes nationales et documents normatifs nationaux 30 pages France.
23. Afnor Editions Normes NF EN 13108-2. 2017. Mélanges bitumineux - Spécifications pour le matériau - Partie 2 : bétons bitumineux très minces BBTM. Normes Francaises et Europiènnes 26 pages France.
24. Correia NS, Zornberg JG. 2014. Influence of tack coat rate on the properties of paving geosynthetics. Transp. Geotech. 1(1):45-54. https://doi.org/10.1016/j.trgeo.2014.01.002.
25. Zhang W. 2017. Effect of tack coat application on interlayer shear strength of asphalt pavement: A state-of-the-art review based on application in the United States. Int. J. Pavement Res. Technol. 10(5):434-445. https://doi.org/10.1016/j.ijprt.2017.07.003.
26. Rahmani A. 2012. Experimental study of the behaviour of a flexible pavement reinforced with a glass fibre-based geogrid. Doctoral thesis. National School of Public Works, Algiers, [s.l.]: [s.n.].
27. Abdessemed M. Kenai S. 2016. Reduction of cracks in airport runways using geogrids. Scientific and technical study day on geosynthetic products ouargla Algeria.
28. Norme ISO 10319. 2015. Géo-synthétiques — Essai de traction des bandes larges.Edition 3. Comité technique ISO / TC 221 Produits géo-synthétiques ICS 59 080 70 Géotextiles.
29. Normes ISO 9864. 2005. Géosynthétiques — Méthode d'essai pour la détermination de la masse surfacique des géotextiles et produits apparentés Comité technique ISO/TC 221. Produits géosynthétiques ICS 59.080.70 Geotextiles.
30. Poulikakos LD, Pittet M, Dumont AG, Partl MN. 2015. Comparison of the two point bending and four point bending test methods for aged asphalt concrete field samples. Mater. Struct. 48:2901–2913. https://doi.org/10.1617/s11527-014-0366-8.
31. Chen L, Qian Zh, Lu Q. 2013. Crack initiation and propagation in epoxy asphalt concrete in the three-point bending test. Road Mater. Pavement Des. 15(3):507-520. https://doi.org/10.1080/14680629.2014.908132.
32. ASTM E2309/E2309M-20. 2020. Standard practices for verification of displacement measuring AFNOR Editions. American Standards ASTM, USA.
33. Afnor Editions Normes NF EN 12697-33. 2020. Mélanges bitumineux - Méthodes d'essai - Partie 33: préparation de corps d'épreuve au compacteur de plaque Normes nationales et documents normatifs nationaux. France.
34. Afnor Editions Normes NF EN 12697-35. 2017. Mélanges bitumineux - Essais - Partie 35 : malaxage de laboratoire Normes nationales et documents normatifs nationaux, France.
35. Afnor Editions Normes BS EN 12697-8. 2019. Matériaux enrobés. Méthodes d'essai Normes anglaises BSI ICS 93.080.20. Matériaux de construction des routes. France.
36. Saride S, Kumar V.V 2017. Influence of geosynthetic-interlayers on the performance of asphalt overlays on pre-cracked pavements. Geotext. Geomembr. 45(3):184-196. https://doi.org/10.1016/j.geotexmem.2017.01.010.

37. Donovan P, Tutumluer R. 2009. Falling weight deflectometer testing to determine relative damage in asphalt pavement unbound aggregate layers. Transp. Res. Rec.: J. Transp. Res. Board. 2104(1):12-23. https://doi.org/10.3141/2104-02.

38. Prayuda H, Kurniawati Djaha SI, Rahmawati H, Monika F, Adly E. 2021. Young's modulus and deflection assessment on pavement using a lightweight deflectometer Int. J. GEOMATE. 20(77):10-17. https://doi.org/10.21660/2020.77.06188.

39. Public transport ministry 2010. Atlas Aéroportuaire/version Zéro, Direction des Infrastructures Aéroportuaires Alger Algérie.

40. Afitex Algeria in French. 2021. Production unit rocessing of non-metallic minerals wood and corkn Kharouba Boumerdes Algeria. Retrieved from http://www.afitexalgerie.com.

41. Pasquini E, Bocci M, Ferrotti G, Canestrari F. 2013. Laboratory characterisation and field validation of geogrid-reinforced asphalt pavements. Road Mater. Pavement Des. 14(1):17-35. https://doi.org/10.1080/14680629.2012.735797.

42. San S, Khazanovich L. 2021. Reconsidering the strength of concrete pavements Int. J. Pavement Eng. 24(2). https://doi.org/10.1080/10298436.2021.2020270.

43. Ingrassia LP, Virgili A, Canestrari F. 2020. Effect of geocomposite reinforcement on the performance of thin asphalt pavements: Accelerated pavement testing and laboratory analysis. Case Stud. Constr. Mater. 12:e00342. https://doi.org/10.1016/j.cscm.2020.e00342.

44. Biligiri KP, Said S, Hakim S. 2012. Asphalt mixtures' crack propagation assessment using semi-circular bending tests. Int. J. Pavement Res. Technol. 5(4):209-217.

45. Ferrotti G, Canestrari F, Pasquini E, Virgili A. 2012. Experimental evaluation of the influence of surface coating on fiberglass geogrid performance in asphalt pavements. Geotext. Geomembr. 34:11-18. https://doi.org/10.1016/j.geotexmem.2012.02.011.

46. Medjdoub A, Abdessemed M. 2023. Tests on the influence of cyclic loading and temperature on the behaviour of flexible pavement reinforced by geogrids with numerical simulation. Tehnički vjesnik. 30(2):521-529. https://doi.org/10.17559/TV-20220806010532.

47. Zhao H, Cao J, Zheng Y. 2014. Investigation of the interface bonding between concrete slab and asphalt overlay. Road Mater. Pavement Des. 18(3):109-118. https://doi.org/10.1080/14680629.2017.1329866.

48. Ragni D, Montillo T, Marradi A, Canestrari F. 2020. Fast falling weight accelerated pavement testing and laboratory analysis of asphalt pavements reinforced with geocomposites Proceedings of the 5th International Symposium on Asphalt Pavements & Environment APE. 417–430.

49. Picoux B, El Ayadi A, Petit C. 2009. Dynamic response of a flexible pavement submitted by impulsive loading. Soil Dyn. Earthq. Eng. 29(5):845-854. https://doi.org/10.1016/j.soildyn.2008.09.001.

50. Ibrahim EM, El-Badawy SM, Ibrahim MH, Gabr A, Azam A. 2017. Effect of geogrid reinforcement on flexible pavements. Innov. Infrastruct. Solut. 2:54. https://doi.org/10.1007/s41062-017-0102-7.

51. Banerjee S, Srivastava MVK, Manna B, Shahu JT. 2022. A novel approach to the designe of geogrid-reinforced flexible pavements. Int. J. Geosynth. Ground Eng. 8:29. https://doi.org/10.1007/s40891-022-00373-3.

52. Noureddine O, Mouloud A, Fouad K. 2022. Static and dynamic behavior of concrete structures reinforced with nanotubes modified composites. Rev. Rom. Mater. 52(1):26–37.

53. Xie T, Qiu YJ. Jiang ZZ, Al CF. 2006. Study on compound type crack propagation behavior of asphalt concrete. Key Eng. Mater. 324-325:759-762. https://doi.org/10.4028/www.scientific.net/KEM.324-325.759.

54. Correia NS, Esquivel ER, Zornberg JG. 2018. Finite-element evaluations of geogrid-reinforced asphalt overlays over flexible pavements. J. Transp. Eng. Part B: Pavements. 144(2):04018020. https://doi.org/10.1061/JPEODX.0000043.

55. Rahman Md M, Saha S, Hamdi ASA, Bin Alam Md J. 2019. Development of 3-D finite element models for geo-jute reinforced flexible pavement. Civ. Eng. J. 5(2):437-446. http://doi.org/10.28991/cej-2019-03091258.

56. Chang DTT, Ho NH, Yi Chang H, Yeh HSh. 1999. Laboratory and case study for geogrid-reinforced flexible pavement overlay. Transp. Res. Rec.: J. Transp. Res. Board. 1687(1):125- 130. https://doi.org/10.3141/1687-14.